Influence of wetting state on optical reflectance spectra of Si nanopillar arrays

Minji Gwon', Sujung Kim', Jiaqi Li, Xiumei Xu, Sun-Kyung Kim, Eunsongyi Lee, Dong-Wook Kim', and Chang Chen'

Citation: J. Appl. Phys. **118**, 213102 (2015); doi: 10.1063/1.4936769
View online: http://dx.doi.org/10.1063/1.4936769
View Table of Contents: http://aip.scitation.org/toc/jap/118/21
Published by the American Institute of Physics

Influence of wetting state on optical reflectance spectra of Si nanopillar arrays

Minji Gwon,[1,a)] Sujung Kim,[1,a)] Jiaqi Li,[2,3] Xiumei Xu,[2] Sun-Kyung Kim,[4] Eunsongyi Lee,[5] Dong-Wook Kim,[1,b)] and Chang Chen[2,3,b)]
[1]*Department of Physics, Ewha Womans University, Seoul 120-750, South Korea*
[2]*imec, Kapeldreef 75, Leuven 3001, Belgium*
[3]*Department of Physics and Astronomy, KU Leuven, Celestijnenlaan 200D, Leuven 3001, Belgium*
[4]*Department of Applied Physics, Kyung Hee University, Gyeonggi-do 446-701, South Korea*
[5]*School of Physics & Astronomy, University of Manchester, Manchester M13 9PL, United Kingdom*

(Received 7 October 2015; accepted 15 November 2015; published online 1 December 2015)

Finite-difference time-domain (FDTD) simulations showed that the reflectance spectra of crystalline Si nanopillar (NP) arrays with diameters of 40, 70, 100, and 130 nm differed depending on wetting state. The observed reflectance dips of the 40-nm-diameter NP array were in good agreement with those estimated from destructive interference conditions at the top and bottom of the NPs: the NP arrays were treated as a homogeneous medium with an effective permittivity according to the effective medium approximation model. In contrast, the dip positions of the FDTD-simulated spectra for 70-, 100-, and 130-nm-diameter NP arrays deviated from the results of interference calculations, particularly for short wavelengths. This suggested that Mie resonances in individual NPs significantly increased the absorption cross-section at the resonant wavelengths, which was sensitive to the refractive index of the surrounding medium (i.e., the wetting state). Optical reflectance measurements provide an easy and efficient means of inspecting the wetting behavior of non-flat surfaces. © *2015 AIP Publishing LLC*. [http://dx.doi.org/10.1063/1.4936769]

I. INTRODUCTION

State-of-the-art semiconductor fabrication techniques enable large-scale production of sub-100-nm Si nanostructure arrays.[1–5] Such progress in nanotechnology requires reliable wet-cleaning processes and methods to inspect the wettability of the nanopatterned Si wafers. The wettability of an ideal smooth surface is often examined using the contact angle of water, which depends on the interfacial energy balance and can be described using Young's equation.[6–9] On the other hand, the wetting behavior of a non-ideal rough surface may deviate significantly from that of a flat surface, requiring sophisticated characterization techniques and careful analyses.[9]

Recently, we proposed that simple optical reflectance measurements could be used to quantitatively determine the instantaneous water imbibition depths and define the actual wetting state on crystalline Si nanopillars (NPs) with diameters of 30–40 nm and a pitch of 90 nm.[3] Proper surface treatments allowed us to control the wetting states of the Si wafers (details can be found in Ref. 3). When complete wetting occurs, water can fill the entire gap between the NPs (see the schematic diagram on the left in Fig. 1(a)). In the case of a non-wetting state, the water droplet can remain on the surface of the substrate and the water imbibition depth is 0 (the right schematic diagram in Fig. 1(a)). The former and latter are called Wenzel and Cassie-Baxter states, respectively.[3]

Si NP arrays exhibit unique optical properties quite distinct from those of their bulk counterparts. The scattering and absorption cross-sections of individual sub-wavelength NPs are much larger than their geometrical cross-section due to Mie resonance.[10–27] The resonance wavelength depends on geometric parameters, such as diameter, length, and pitch of the array. As a result, NPs with different dimensions can display various colors.[10–17] In addition, the Mie resonance as well as the gradual decrease of the refractive index and multiple scattering of the NP array enables broad-band and omnidirectional antireflection (AR) effects.[18–25] NP arrays also can exhibit the second-order-scattering-induced reflection divergence and nonlinear depolarization[26] and enhanced Stoke Raman scattering.[27] Therefore, varying geometrical

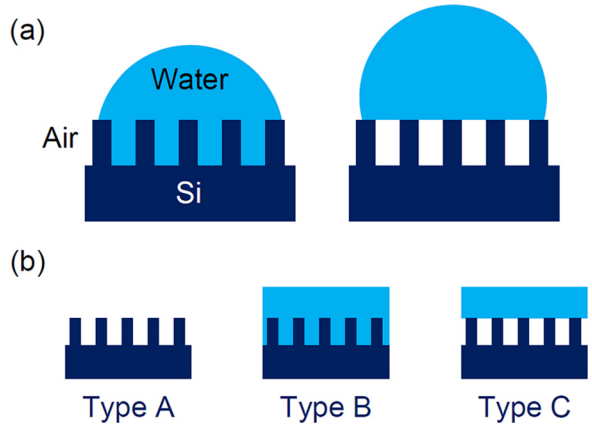

FIG. 1. (a) Schematic illustrations depicting two distinct wetting states of NP arrays. (b) Three types of arrays used in the simulations. Type-A corresponds to NPs in air, type-B to NPs completely immersed in water, and type-C corresponds to NPs immersed in water but with air filling the gaps between neighboring NPs.

[a)]M. Gwon and S. Kim equally contributed to this work.
[b)]Electronic addresses: dwkim@ewha.ac.kr and change.chen@imec.be

configurations of the NP array will significantly modify their optical characteristics. This will make the inspection on the wetting status through optical reflectance even more complex, and requires a systematic study on the influence of wetting states on the optical characteristics of Si NP arrays with various diameters and pitches.

In this article, we report a finite-difference time-domain (FDTD) simulation study of the optical characteristics of Si NP arrays in air and water, using NPs with a range of diameters (40, 70, 100, and 130 nm) and pitches. While our earlier work focused only on Si NPs with diameters of 30–40 nm where no Mie resonance is allowed for wavelengths (λ) > 400 nm,[3] this study extends the work to cover Si NPs with larger diameters where leaky Mie resonances may affect their reflectance spectra. The FDTD simulated reflectance spectra were compared with the effective medium approximation (EMA) model, in which the NP array plane was treated as a homogeneous medium with an effective permittivity. The EMA model can be exploited for rapid identification of reflectance dips to first-order, prior to more sophisticated full-vectorial numerical simulations. By conducting FDTD simulations with respect to different media surrounding NP arrays, we discovered that optical reflectance measurements can be used to inspect the wetting states of NP arrays, regardless of the NP diameter.

II. RESULTS AND DISCUSSION

A. Interference: Effective medium approximation

As written above, schematic diagrams shown in Fig. 1(a) depict two distinct wetting states of NP arrays. To investigate the optical spectral response of NP arrays, three types of array were considered, as shown in Fig. 1(b). Type A is an NP array in air and type B is an NP array completely immersed in water. Type C is an NP array immersed in water, while air remains in the gaps between neighboring NPs.

When the diameter of the NPs (D) was smaller than approximately 50 nm, no leaky waveguide modes were observed in the wavelength range of 400–1000 nm.[17] Therefore, for $D < 50$ nm, the NPs and surrounding media may be considered an optically homogeneous medium with an effective refractive index n_{eff} based on the EMA model.[24,28] As a result, incident light will undergo reflections at the air–NP and NP–substrate interfaces, resulting in interference, as illustrated in Fig. 2.

According to EMA theory, ε_{eff} is a function of the permittivity of the suspending medium ε_{m}, the permittivity of embedded spheres ε, and the volume fraction of the spheres f

$$\frac{\varepsilon_{eff} - \varepsilon_m}{\varepsilon_{eff} + 2\varepsilon_m} = f\frac{\varepsilon - \varepsilon_m}{\varepsilon + 2\varepsilon_m}. \quad (1)$$

A similar relation applies for a mixture of parallel circular cylinders, such as the NP arrays discussed here, and the surrounding medium.[28] With our NP arrays, $n_{eff} = \sqrt{\varepsilon_{eff}}$, where ε_{m} is the dielectric constant of the surrounding medium (air or water, see Fig. 1(b)), ε is the dielectric constant of Si, and f is equal to $\frac{\pi D^2}{4P^2}$ where P is the pitch of the NP array.

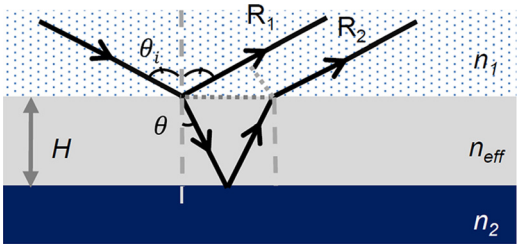

FIG. 2. Schematic diagram illustrating interference phenomena in the NP arrays. Here, n_1, n_{eff}, and n_2 are the refractive indices of the region above the NPs, the NP-and-medium, and the underlying Si substrate, respectively. H, θ_i, and θ are the height of the NPs, the incident angle of light, and the angle of refraction of light, respectively. R_1 and R_2 indicate light rays reflected at the top and bottom of the NPs.

The type-A and type-B NPs are in air and fully immersed in water, respectively, so $n_{\text{air}} < n_{\text{eff}} < n_{\text{Si}}$ and $n_{\text{water}} < n_{\text{eff}} < n_{\text{Si}}$. The type-C NPs were immersed in water, but the gaps were filled with air, and so $n_{\text{eff}} < n_{\text{water}} < n_{\text{Si}}$ for small D/P and $n_{\text{water}} < n_{\text{eff}} < n_{\text{Si}}$ for large D/P. Light undergoes a phase shift of π when incident light passing through a medium with a smaller refractive index is reflected at the surface of a medium with a larger refractive index. Considering such a phase shift, the destructive interference wavelength λ_{dip} corresponding to the resulting dip in reflectance is given by

$$\lambda_{dip} = n_{eff}\frac{4H}{2m+1}\cos\theta \quad (2)$$

for n_{air} (or n_{water}) < $n_{\text{eff}} < n_{\text{Si}}$ and

$$\lambda_{dip} = n_{eff}\frac{4H}{2m}\cos\theta \quad (3)$$

for $n_{\text{eff}} < n_{\text{water}} < n_{\text{Si}}$, where m is a positive integer, H is the height of the NPs, and θ is the angle of refraction (Fig. 2). Equation (2) is valid for type-A and type-B NPs, and for type-C NPs with large D/P. Equation (3) is valid for type-C NPs with small D/P.

B. Optical simulation method

We carried out FDTD simulations using Lumerical FDTD Solutions version 8.7.4 (Lumerical Solutions, Vancouver, BC, Canada) to investigate the optical spectral response of the three kinds of NP arrays (Fig. 1(b)). The FDTD calculations[15–22] as well as the rigorous coupled-wave analyses[24,25] have successfully explained the omnidirectional antireflection effects of sub-wavelength-sized NP arrays. A cylindrical crystalline Si NP array on the same Si substrate was studied; the height, H, was 420 nm, the diameters of the NPs were $D = 40$, 70, 100, and 130 nm, and the pitch P was varied such that $0.1 \le D/P \le 0.7$. Periodic boundary conditions were used along the in-plane directions, and perfectly matched layers (PML) were used as the radiation boundary condition at the top and bottom of the simulated structure. A plane wave light source was used, and the wavelength was varied from 400 nm to 1000 nm in 91 wavelength steps. Monitors for collecting reflected light were placed above the plane wave and the optical reflectance was calculated by

dividing the reflected light intensity by the incident light intensity generated from the plane wave. Note that the reflectance includes both specular and diffuse light. The dispersion characteristics of crystalline Si were used for the FDTD simulations.[29] For type-B and type-C NP arrays, the ambient medium was set to be water (i.e., a plane wave generated in water) because in wetting experiments, the water ambient medium had a thickness of a few mm,[3] which is far higher than the coherence length of the incident light, such that the air-water interface would not affect the reflection spectra of the NP arrays. The reflectance spectra, obtained from the FDTD simulations, were plotted as a function of the wavelength in vacuum and can be readily compared with experimental data.[3]

C. Reflectance spectra of 40-nm-diameter nanopillar arrays

Figure 3 shows the simulated reflectance spectra for type-A, type-B, and type-C NP arrays with $D = 40$ nm. The spectra for all three types of NP array with the same P value exhibited distinct trends, depending on the wetting states. The expected interference-dip wavelengths (λ_{dip}), calculated from Eqs. (2) and (3), are indicated as symbols in the reflectance curves in Fig. 3. For the estimation of λ_{dip}, the refractive index of water was set to be 1.33. In the case of Si, the average refractive index across the wavelength range from 400 nm to 1000 nm was used for simple calculations. The largest difference between λ_{dip} estimated using the average index of refraction and that from the exact refractive index was ~20 nm. The dips of the FDTD reflectance spectra are in good agreement with the interference dips of all three types of NP array for a range of D and P. In addition, for the type-A and type-B NP arrays, the reflectance spectra became less structured with increasing P (i.e., decreasing volume fraction of Si). For example, the reflectance spectra with $P = 400$ nm simply obeys the material dispersion characteristics of crystalline Si.[29] In contrast, for the type-C array, relatively pronounced dips were observed even for $P = 200$ and 400 nm. We postulate that the high-contrast dips result from an increase in refractive index difference between the Si NP array plane (Si + air) and the ambient medium (water). These numerical findings suggest that simple reflectance measurements and interference analyses could be useful for inspecting the wetting states of NP arrays with such small diameters.[30]

D. Reflectance spectra of 70-, 100-, and 130-nm-diameter nanopillar arrays

Figure 4 shows the FDTD-simulated reflectance curves of type-A, type-B, and type-C NP arrays with $D = 70$, 100, and 130 nm. For the NPs with $D = 70$ nm, the FDTD reflectance dips at long wavelengths are still well matched with those predicted from the EMA model. However, the EMA model fails to account for the dips at short wavelengths. Note that the FDTD reflectance of 70-nm-diameter NPs with large $P = 233$ and 350 nm clearly exhibit dips at $\lambda \sim 450$ nm. These dips are attributed to excitation of the fundamental (HE_{11}) waveguide mode[15] and resulting enhancement of the absorption cross-section of the NPs.[10–22] The electric field of the fundamental mode is strongly localized at the core of the NPs, as shown in Figs. 5(a) and 5(b). As a result, the dip position does not change much due to either the presence of the substrate or the wetting state.

The NPs with $D = 40$ nm cannot support Mie resonance at $\lambda > 400$ nm,[15] and hence interference is the dominant effect in the reflectance spectra. The Mie resonance dips for larger D shift monotonically to longer wavelengths; dips appear (HE_{11} mode) at $\lambda \sim 600$ nm for $D = 100$ nm, and two dips were observed (HE_{11} and HE_{21} modes) at $\lambda \sim 400$ and ~700 nm for $D = 130$ nm.[15] Mie resonance results in enhanced light absorption and a reflection dip, as shown in Fig. 4. Note that the Mie resonance dips split and broaden with decreasing P (i.e., increasing filling fraction of the NPs). This indicates optical coupling between neighboring NPs, as reported earlier.[15–17] The refractive index of the surrounding medium may alter the evanescent field tails outside of the NPs and the difference in the field patterns can be noted in type-A and type-B NP arrays (Figs. 5(a) and 5(b)). Thus, wettability can affect the coupled modes between neighboring NPs. This explains the distinct reflectance spectra observed for the NP arrays depending on their wetting state, even for short wavelengths, as shown in Fig. 4.

IV. CONCLUSION

We demonstrated that simple optical reflectance measurements can be used to determine the wettability of vertically oriented NP arrays with various diameters and pitches. The spectra calculated using FDTD simulations for small

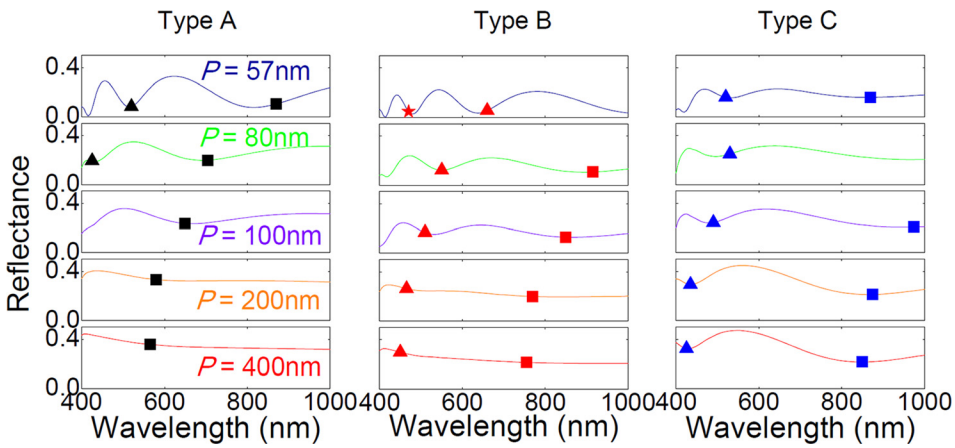

FIG. 3. FDTD-simulated reflectance spectra of 40-nm-diameter NP arrays with different wetting states. The symbols in the reflectance spectra indicate the dips expected from destructive interference conditions (calculated using Eqs. (2) and (3)).

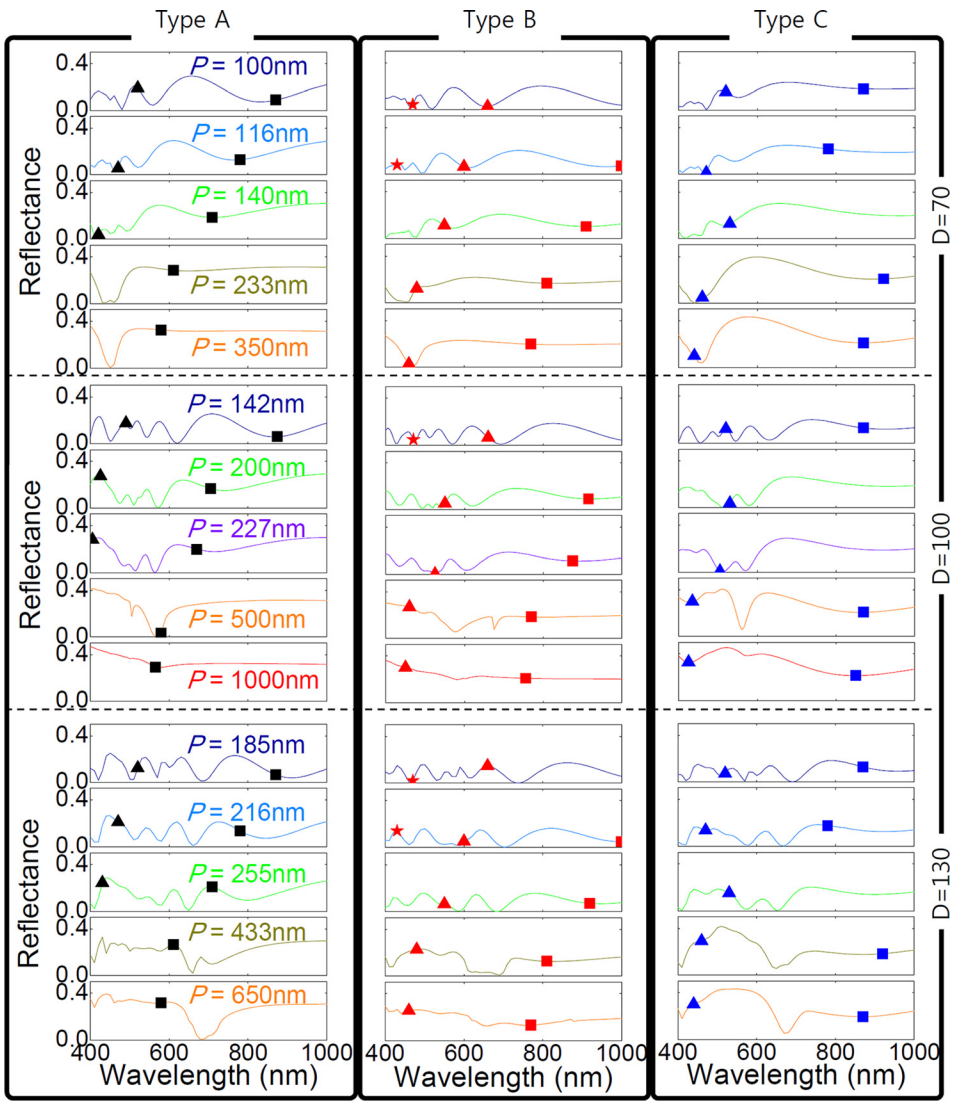

FIG. 4. The simulated reflectance spectra of NP arrays with different diameters (70, 100, and 130 nm). The symbols indicate the dips expected from destructive interference conditions (i.e., calculated using Eqs. (2) and (3)). Curves of the same color have identical D/P.

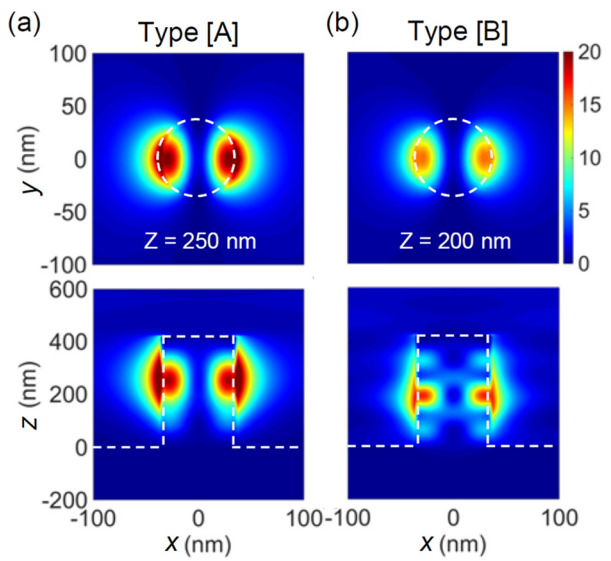

FIG. 5. Electric field intensity ($|E/E_0|^2$) plots of (a) type-A and (b) type-B NP arrays with diameters of 70 nm at $\lambda = 450$ nm. E_0 indicates the magnitude of the incident plane wave.

diameter NPs are well described by interference at the top and bottom of the NPs and the NP-air/water region can be regarded as a homogenous medium with an effective refractive index. Large diameter NPs show Mie resonance in the visible wavelength range, and hence, in addition to interference, their reflectance spectra can be explained by excitations of leaky Mie resonances in the NPs.

ACKNOWLEDGMENTS

This work was supported by New & Renewable Energy Technology Development Program of the Korea Institute of Energy Technology Evaluation and Planning (KETEP) Grant (No. 20123010010160) and Basic Science Research Programs through the National Research Foundation of Korea Grant (Nos. NRF-2013R1A1A2063744 and NRF-2013R1A1A1059423). C.C. acknowledges the financial support from the FWO (Flanders) of Belgium (12D4112N).

[1]I. Vos, D. Hellin, J. Vertommen, M. Demand, and W. Boullart, ECS Trans. **41**, 189 (2011).
[2]J. Li, C. Chen, H. Jans, X. Xu, N. Verellen, I. Vos, Y. Okumura, V. V. Moshchalkov, L. Lagae, and P. V. Dorpe, Nanoscale **6**, 12391 (2014).
[3]X. Xu, G. Vereecke, C. Chen, G. Pourtois, S. Armini, N. Verellen, W.-K. Tsai, D.-W. Kim, E. Lee, C.-Y. Lin, P. Van Dorpe, H. Struyf, F.

Holsteyns, V. Moshchalkov, J. Indekeu, and S. De Gendt, ACS Nano **8**, 885 (2014).
[4]G.-R. Lin, C.-J. Lin, H.-C. Kuo, H.-S. Lin, and C.-C. Kao, Appl. Phys. Lett. **90**, 143102 (2007).
[5]G.-R. Lin, Y.-H. Pai, and C.-T. Lin, J. Lightwave Technol. **26**, 1486 (2008).
[6]P. G. de Gennes, Rev. Mod. Phys. **57**, 827 (1985).
[7]D. Quéré, Rep. Prog. Phys. **68**, 2495 (2005).
[8]X. Feng and L. Jiang, Adv. Mater. **18**, 3063 (2006).
[9]D. Bonn, J. Eggers, J. Indekeu, J. Meunier, and E. Rolley, Rev. Mod. Phys. **81**, 739 (2009).
[10]L. Cao, J. S. White, J.-S. Park, J. A. Schuller, B. M. Clemens, and M. L. Brongersma, Nat. Mater. **8**, 643 (2009).
[11]K. Seo, M. Wober, P. Steinvurzel, E. Schonbrum, Y. Dan, T. Ellenbogen, and K. B. Crozier, Nano Lett. **11**, 1851 (2011).
[12]B. C. P. Sturmberg, K. B. Dossou, L. C. Botten, A. A. Asatryan, C. G. Poulton, C. M. de Sterke, and R. C. McPhedran, Opt. Express **19**, A1067 (2011).
[13]M. Khorasaninejad, N. Abedzadeh, J. Walia, S. Patchett, and S. S. Saini, Nano Lett. **12**, 4228 (2012).
[14]S. Wells, I. A. Merkulov, I. I. Kravchenko, N. V. Lavrik, and M. J. Sepaniak, ACS Nano **6**, 2948 (2012).
[15]B. Wang and P. W. Leu, Opt. Lett. **37**, 3756 (2012).
[16]F. J. Bezares, J. P. Long, O. J. Glembocki, J. Guo, R. W. Rendell, R. Kasica, L. Shirey, J. C. Owrutsky, and J. D. Caldwell, Opt. Express **21**, 27587 (2013).
[17]C. Wang, Z. Y. Jia, K. Zhang, Y. Zhou, R. H. Fan, X. Xiong, and R. W. Peng, J. Appl. Phys. **115**, 244312 (2014).
[18]P. Spinelli, M. A. Verschuuren, and A. Polman, Nat. Commun. **3**, 692 (2011).
[19]P. Krogstrup, H. I. Jørgensen, M. Heiss, O. Demichel, J. V. Holm, M. Aagesen, J. Nygard, and A. F. Morral, Nat. Photon. **7**, 306 (2013).
[20]X. Zhang, C. W. Pinion, J. D. Christesen, C. J. Flynn, T. A. Celano, and J. F. Cahoon, J. Phys. Chem. Lett. **4**, 2002 (2013).
[21]K.-D. Song, T. J. Kempa, H.-G. Park, and S.-K. Kim, Opt. Express **22**, A992 (2014).
[22]S.-K. Kim, X. Zhang, D. J. Hill, K.-D. Song, J.-S. Park, H.-G. Park, and J. F. Cahoon, Nano Lett. **15**, 753 (2015).
[23]G.-R. Lin, Y.-C. Chang, E.-S. Liu, H.-C. Kuo, and H.-S. Lin, Appl. Phys. Lett. **90**, 181923 (2007).
[24]S.-H. Hsu, E.-S. Liu, Y.-C. Chang, J. N. Hilfiker, Y. D. Kim, T. J. Kim, C.-J. Lin, and G.-R. Lin, Phys. Stat. Sol. (a) **205**, 876 (2008).
[25]F.-S. Meng, Y.-H. Lin, and G.-R. Lin, J. Appl. Phys. **109**, 083523 (2011).
[26]G.-R. Lin, F.-S. Meng, and Y.-H. Lin, Prog. Electromagn. Res. **117**, 67 (2011).
[27]G.-R. Lin, Y.-H. Lin, Y.-H. Pai, and F.-S. Meng, Opt. Express **19**, 597 (2011).
[28]O. S. Heavens, *Optical Properties of Thin Solid Films* (Dover, New York, 1991).
[29]W. M. Haynes, *CRC Handbook of Chemistry and Physics* (CRC Press, 2015).
[30]See supplementary material at http://dx.doi.org/10.1063/1.4936769 for comparison of experimental and calculated optical reflectance spectra of the NP arrays with distinct wetting states.